Biophysical Chemistry 182 (2013) 64–70

Contents lists available at ScienceDirect

Biophysical Chemistry

journal homepage: http://www.elsevier.com/locate/biophyschem

What planar lipid membranes tell us about the pore-forming activity of cholesterol-dependent cytolysins

Marta Marchioretto [a,b], Marjetka Podobnik [c], Mauro Dalla Serra [a,*], Gregor Anderluh [c,d,e,**]

[a] National Research Council — Institute of Biophysics & Bruno Kessler Foundation, Via alla Cascata 56/C, 38123 Trento, Italy
[b] University of Trento, Via Belenzani 12, 38122 Trento, Italy
[c] National Institute of Chemistry, Hajdrihova 19, 1000 Ljubljana, Slovenia
[d] Department of Biology, University of Ljubljana, Večna pot 111, 1000 Ljubljana, Slovenia
[e] En-Fist Centre of Excellence, Dunajska cesta 156, Ljubljana, Slovenia

HIGHLIGHTS

- Pore-forming toxins (PFTs) are used for attack and defense by many organisms.
- Cholesterol-dependent cytolysins (CDCs) are an important toxin family from bacteria.
- The planar lipid membrane approach provides information on activity of PFTs.
- Published studies of CDC reflect different ways on how pores are formed.

GRAPHICAL ABSTRACT

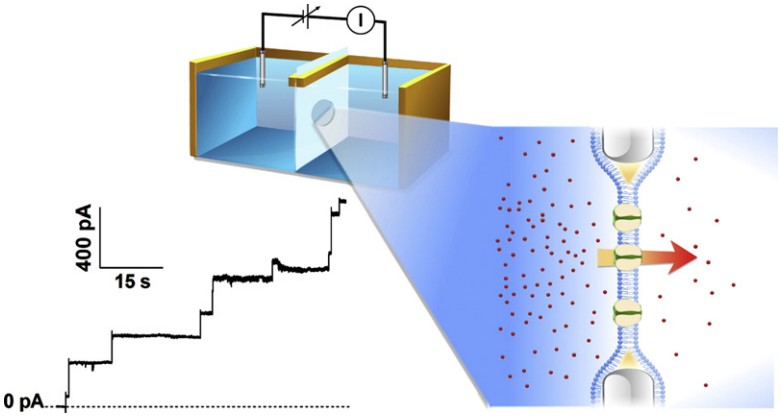

ARTICLE INFO

Article history:
Received 9 May 2013
Received in revised form 19 June 2013
Accepted 19 June 2013
Available online 2 July 2013

Keywords:
Cholesterol-dependent cytolysin
Listeriolysin O
Perfringolysin O
Planar lipid membranes
Pore-forming toxin
Pore

ABSTRACT

Pore-forming toxins are an important group of natural molecules that damage cellular membranes by forming transmembrane pores. They are used by many organisms for attack or defense and similar proteins are employed in the immune system of vertebrates. Various biophysical approaches have been used to understand how these proteins act at the molecular level. One of the most useful, in terms of monitoring pore formation in real time, is a method that employs planar lipid membranes and involves ionic current measurements. Here we highlight the advantages and possibilities that this approach offers and show how it can advance understanding of the pore-forming mechanism and pore properties for one of the most important families of natural toxins, the cholesterol-dependent cytolysins.

Abbreviations: AFM, atomic force microscopy; CDC, cholesterol-dependent cytolysins; Chol, cholesterol; D, domain; DOPC, 1,2-dioleoyl-*sn*-glycero-3-phosphocholine; DPhPC, 1,2-diphytanoyl-*sn*-glycero-3-phosphocholine; Hepes, N-2-hydroxyethylpiperazine-N′-2-ethanesulphonic acid; LLO, listeriolysin O; PC, phosphatidylcholine; PFO, perfringolysin O; PFT, pore-forming toxin; PLM, planar lipid membrane; PLY, pneumolysin; POPC, 1-palmitoyl-2-oleoyl-*sn*-glycero-3-phosphocholine; TMH, transmembrane β-hairpin; Tris, tris(hydroxymethyl)aminomethane; MES, 2-(N-morpholino)ethanesulfonic acid.

* Correspondence to: M. Dalla Serra, National Research Council — Institute of Biophysics & Bruno Kessler Foundation, via alla Cascata 56/C, 38123 Trento, Italy. Tel.: +39 0461 314156.
** Correspondence to: G. Anderluh, National Institute of Chemistry, Hajdrihova 19, 1000 Ljubljana, Slovenia. Tel.: +386 1 476 02 61.
E-mail addresses: mauro.dallaserra@cnr.it (M. Dalla Serra), gregor.anderluh@ki.si (G. Anderluh).

0301-4622/$ – see front matter © 2013 Elsevier B.V. All rights reserved.
http://dx.doi.org/10.1016/j.bpc.2013.06.015

1. Introduction

Pore-forming toxins (PFTs) are an important class of proteins produced mainly by bacteria, where they constitute the biochemical arsenal for attack or defense. PFTs are secreted as monomeric, water soluble proteins that oligomerize on the target cell membrane, thereby producing structured, nanometer-size pores (reviewed in [1–4]). Well-studied PFT families include aerolysin and related toxins, staphylococcal α-toxin and related toxins, cholesterol-dependent cytolysins (CDCs), colicins, actinoporins from sea anemones, and others [1,3]. PFTs induce cell death, either by directly impairing cell membrane integrity or by facilitating internalization of other toxic molecules. Much effort has been devoted to visualizing their structure directly and clarifying the mechanism of pore assembly on cell membranes. Pore-forming activity can easily be investigated by determining red blood cell hemolysis or the release from cells of lactate dehydrogenase, as well as by the more sophisticated electrophysiological technique of patch-clamp. The use of well characterized lipid membrane model systems has been employed successfully with PFTs, since the oligomerization of monomers and the coordinated conformational changes leading to assembly of pores are often triggered solely by the presence of a lipid bilayer. All environmental conditions can be finely controlled and changed with lipid model systems, which therefore become very useful and significant cell-membrane mimicking systems. Liposomes have been used in leakage assays to study membrane permeabilization, investigate special lipid requirements, estimate pore dimensions, etc. (reviewed in [5]). Electrophysiology on planar lipid membranes (PLM) has been extensively engaged for the functional characterization of many membrane interacting proteins and peptides, including PFTs as outlined below and in [6]. In this review we present (i) the PLM approach for studying the properties of pores and mechanism of pore formation, (ii) CDC protein family and (iii) how PLM helps to understand the pore-forming activity of CDCs.

2. Measuring pores directly

PLM is a highly sensitive method that enables single channel openings to be studied in real time (reviewed in [6,7]). The technique includes recording the ionic current passing through a stable lipid bilayer of controlled lipid composition. Typically, the bilayer is formed on a small aperture (100 μm diameter) made in a thin (25 μm) Teflon septum separating two chambers. The two chambers mimic the intra- and extra-cellular spaces. They are filled with an ionic solution and connected to an electronic system with two Ag–AgCl electrodes that permit the application of a stable electrical potential (in the range of tens of mV) and the recording of the ionic current passing through the membrane. The protein, added in one chamber only, can interact with the phospholipid bilayer, oligomerize and form pores (Fig. 1A). Typically, each single pore is detected in real time as an abrupt increase in the current. Successive pore insertions produce characteristic, step-like increments in current, as highlighted in Fig. 1B. PLM is a single molecule technique since each jump corresponds to the opening of a single active pore.

PLM allows several parameters that could influence PFT activity to be readily controlled and varied. Lytic ability of toxins can be observed under various environmental conditions, like salt concentration and composition, pH, temperature, transmembrane potential, as well as membrane lipid composition (either in a symmetric or asymmetric leaflet configuration). Any structural–functional correlation can be highlighted by including binding molecules and/or potential inhibitors of toxin activity.

PLM allows characteristic biophysical features of the pore to be determined, such as its size, ionic selectivity and voltage dependence. Pore size can be estimated from the single pore conductance (G), defined as the ratio of the amplitude of a single current jump (I) to the applied potential (V). Considering the pore as a cylindrical hole, its conductance is directly proportional to the pore area, as expressed in Eq. (1)

$$G = \frac{\sigma A}{L}, \tag{1}$$

where A is the area of the pore, L its length, and σ the conductivity of the buffer.

Pore selectivity can be analyzed by measuring the reversal potential, i.e. the electrical potential giving zero current, under asymmetric buffer conditions (e.g. different salt concentrations in the two chambers). Using the standard Goldman–Hodgkin–Katz equation [7], the permeability ratio between cations and anions (P_{K^+}/P_{Cl^-}) can be calculated as:

$$\frac{P_{K^+}}{P_{Cl^-}} = \frac{[a_{Cl^-}]_t - [a_{Cl^-}]_c\, e^{\frac{FV_{rev}}{RT}}}{[a_{K^+}]_t\, e^{\frac{FV_{rev}}{RT}} - [a_{K^+}]_c} \tag{2}$$

where RT/F is 25 mV at room temperature, V_{rev} is the reversal potential, a_i is the activity of ion i, and c and t correspond to the *cis* and *trans* chambers.

PLM can also be used to monitor the transport of macromolecules through the pores [8–10]. In this way, neutral polymers may be detected during their partition into the nanopore lumen. The decrease in the ionic current is related to polymer dimensions and provides information on the geometry of the pore [11]. The introduction of large molecules into the pore lumen may serve as convenient molecular adapters for increasing the sensitivity of detection of small specific analytes [12]. Interestingly, DNA can also be detected by nanopores reconstituted in PLM. The first and simplest approach for DNA sequencing is to transfer the charged molecule through the pore, driven by an applied electric potential. The passage of each nucleotide through the narrowest pore restriction partially occludes the pore, causing a characteristic reduction of the ionic current. The improved nanopore-based approaches exploit different chemical modifications or protein-derivatized nanopores in order to increase the yield of nucleotide transfer through the pore and to increase the residence time for permitting a more robust base recognition. In particular, an exonuclease has been linked to the top of the pore, allowing more specific interaction with DNA and the release of single nucleotides inside the pore [13]. Alternatively, a polymerase protein placed in the upper part of the pore structure has been used to synthesize a new RNA molecule from the template, thus releasing specific tags inside the pore [14]. More recently, nanopore technology has been exploited for protein detection [15] and drug screening. There have been some improvements on how this single molecule approach can be used in biomedical applications in high-throughput format, creating a nanopore 'micro-chip'. Another recent PLM application is the development of microfluidic devices that allow easier manipulation of environmental conditions (e.g. buffer exchange [16]) and also permit parallelization for drug screening at the single pore level [17]. The use of hydrogels is becoming popular for stabilizing the membrane bilayer in the devices. The hydrogel supported membrane itself becomes a micro-system for pore-forming studies at the molecular level, and even at the optical level [18], as well as for mimicking the electrical circuit [19]. The recently developed nanodroplet approach enables simultaneous optical and electrophysiological detection of single pores and ion movements (e.g. movements of Ca^{2+} ions through a single α-toxin pore [20]) and kinetics of multimeric pore assembly [21]. The nanodroplet system has been used by Fischer and coworkers to provide an elegant demonstration of transport of a macromolecular lethal factor through a single anthrax protective antigen pore [22].

A technique that allows simultaneous electrophysiological and structural analyses would be an effective method by which to study the mechanism of CDCs and PFT pore-formation. However, this remains a significant challenge. At present, the best option is to

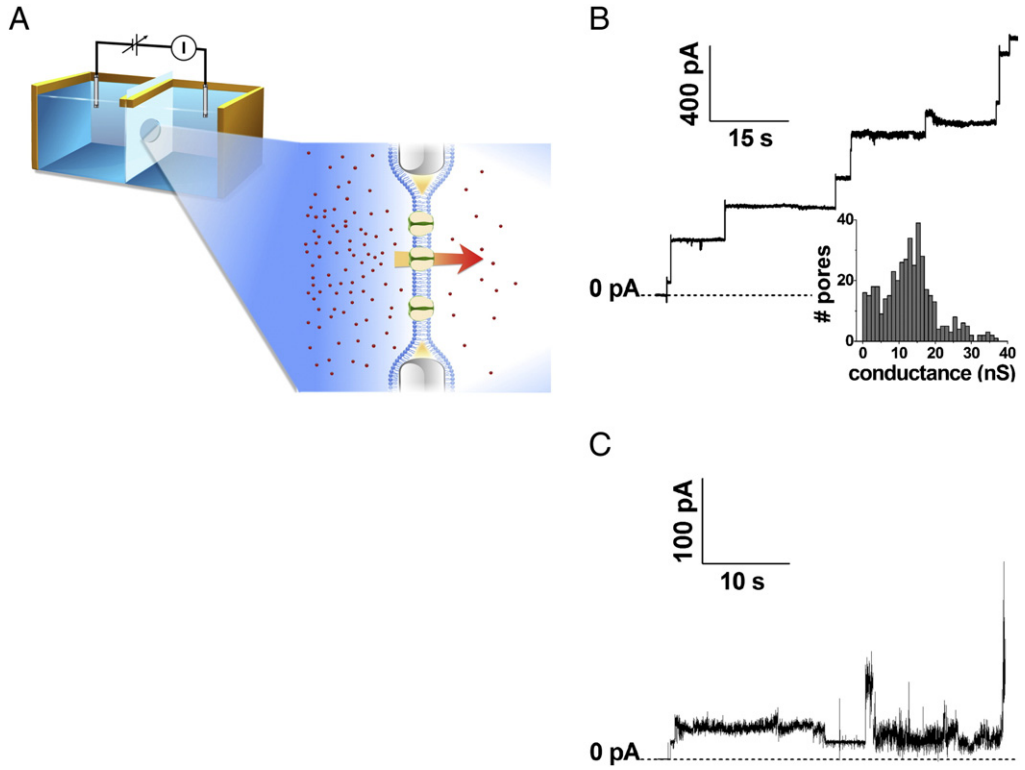

Fig. 1. Planar lipid membranes provide a tool to monitor pore formation. (A) Scheme of a typical PLM setup. Two chambers made of Teflon are separated by a holed septum over which the bilayer is formed. Two Ag/AgCl electrodes are inserted into the two compartments, *cis* (left side, where protein is added) and *trans* (right side) for applying the desired electrical potential and, at the same time, measuring the current flowing through the membrane. A pore-forming protein is added into the *cis* compartment only and, when a single pore is formed, a sudden step-like increase in the current is usually recorded (as reported in B and C). The current trace reported in panel C follows a different behavior, normally ascribed to less structured openings, as already reported for some CDC (Table 1). (B) An example of formation of a defined pore, identified by the characteristic step-like increase in the current trace. Pores are formed by CDC Perfringolysin O from *Clostridium perfringens* (12 nM) on a POPC:CHO 1:1 membrane. The bath solution was 100 mM KCl, 20 mM Hepes pH 7.4, and the applied potential +40 mV. The cumulative histogram of the conductances is shown in the inset. The resulting mean conductance value is 14.2 ± 3.7 nS. (C) An example of a noisy trace, with smaller step-like increases, produced by CDC Listeriolysin O from *Listeria monocytogenes* (10 nM) on a DOPC:CHO 4:1 membrane. The bath solution was 10 mM MES pH 5.5, 100 mM KCl and the applied potential +40 mV. The different current increases shown in B and C reflect two different ways by which pores are formed on the membrane.

combine results obtained by the two methods separately, in order to assign a specific pore structure to the lytic activities recorded on PLM. Structural data are essential to understand the protein rearrangement during protein insertion, but only with the PLM technique is it possible to monitor the pore opening in real time, by following the kinetics of pore-formation and thus understanding the various ways in which PFTs can form pores.

3. Cholesterol-dependent cytolysins constitute a model system for PFTs

CDCs are one of the most important groups of natural toxins. They are produced by many genera of pathogenic Gram-positive bacteria and are considered to be important virulence factors (reviewed in [23]). However, beyond their role of targeting and destroying biological membranes, these toxins are potent regulators of the host cell signaling and immunity [24]. The mechanism of pore formation in biological membranes has also been used to improve drug delivery [25,26]. More than 20 different CDCs have been described, including perfringolysin (PFO) from bacteria *Clostridium perfringens*, pneumolysin (PLY) from *Streptococcus pneumonia* and listeriolysin O (LLO) from *Listeria monocytogenes* [23,27]. Interestingly, CDCs are encoded only by those Gram-negative bacteria that lack a pathogenic interaction with animals, while the CDC genes are absent from the genomes of Gram-negative pathogens. Hotze et al. (2013) hypothesize that this group of CDCs represent a bacterial defense system against bacterial predators such as protozoa [28].

CDCs are probably the best studied of the PFT families. Intensive research over the last two decades has enabled a precise description of how they interact with lipid membranes and oligomerize at the membrane surface, thus forming a pre-pore complex that is finally transformed into a large, transmembrane pore by bringing specific regions of each monomer across the lipid membrane [2,23,27,29]. Pore formation of most CDCs depends completely on the presence of cholesterol as a receptor in the membranes, with the exception of three members (intermedilysin [30], vaginolysin [31] and lectinolysin [32]) that also require the presence of protein receptor CD59 or carbohydrates. The pores formed by CDCs are very large, among the largest in the PFT world. They are built of 35–40 monomers, resulting in a pore with a diameter of 25–30 nm.

The members of the CDC family encoded by Gram-positive bacteria are highly similar in primary structure, with 40 to 70% identity of amino acid residues. They are secreted from bacterial cells as soluble monomers, using a typical type II signal peptide. The only known exception to this rule is PLY whose release from the bacterium in the absence of a propeptide is still unexplained (reviewed in [23]). The type II signal peptide is absent from CDCs from Gram-negative bacteria [28].

The molecular weights of mature CDCs range from 50 to 72 kDa. This broad range is due mostly to differences in the length of their N-terminal extensions, which may be as great as 150 residues. The part of the CDC polypeptide chain involved in pore formation is around 50 kDa. The monomeric form of PFO was the first CDC to be crystallized and its crystal structure [33] showed that a CDC molecule is organized in four domains (D1 to D4) (Fig. 2A). Crystal structures of three other CDC family members

have been determined: intermedilysin from *Streptococcus intermedius* [34], anthrolysin O from *Bacillus anthracis* [35], and suilysin from *Streptococcus suis* [36]. All these structures have very similar folds, with domain D4 as the most exposed domain in the structure of the CDC monomer (Fig. 2). The tip of domain D4 mediates the attachment of CDC monomers to the membrane (Fig. 2A and B). It contains a conserved undecapeptide, a tryptophan rich motif of 11 amino acid residues, and three adjacent loops (L1, L2, L3) with several conserved residues that promote interactions with the membrane cholesterol (Chol) [37,38]. Oligomerization to a pre-pore complex at the surface of the membrane is mediated mostly by contacts through domain D1. Domain D3, which comprises approximately 25% of residues of the CDC polypeptide chain (as in PFO), is the part of the structure that undergoes the most dramatic conformational change at the final step that includes a collapse of the membrane attached pre-pore into a transmembrane pore (Fig. 2B). In the monomeric form of CDCs, D3 contains two bundles of α-helices that, during pore formation, are structurally transformed into two transmembrane β-hairpins (termed TMH1 and TMH2, comprising approximately 12% of the residues in PFO), which constitute the central building block of the β-barrel pore contributed by each monomer (Fig. 2B). Domain D2 is a linker domain, providing the structural flexibility that is required in the rearrangement of D3, and bringing the transmembrane β-hairpins across the membrane. On transition to the pore, the oligomeric complex undergoes a 4 nm vertical collapse to insert the β-barrel pore into the bilayer [39], involving a dramatic disruption of the D2–D3 interface.

Recent structural work on another family of pore-forming proteins, the MACPF domain proteins, showed unexpected structural similarity to CDCs [40], however, although without any sequence similarity. The MACPF family of pore-forming proteins initially included proteins of the membrane attack complex (MAC) and perforin, but now contains many other proteins from eukaryotes and prokaryotes. Eukaryotic MACPF proteins have been shown to function in immunity, invasion and development, through either lytic or non-lytic mechanisms [27,41]. Crystal structures of MACPF family members show a striking similarity to the fold of domains D1 and D3 of CDCs. This part of the molecule thus functions as a single operational unit, and both protein families are now collectively referred to as the MACPF/CDC superfamily. Due to this structural similarity it has been suggested that members of the MACPF protein family form pores by a mechanism similar to that of CDCs. There is, however, little functional evidence to support such a proposition [27,41].

Cryo-electron microscopy, atomic force microscopy (AFM), and planar lipid membrane studies on pore formation by MACPF/CDC superfamily members has provided important insights into the mechanism of pore formation and the properties of the pores. It was shown that fully formed circular proteinaceous pores and transmembrane arcs and double arc pores coexist (reviewed in [29,42]) (Fig. 2C). Arcs were proposed to be smaller transmembrane proteolipidic pores lined by a protein oligomer on one side and lipids on the other. These arcs may not be experimental artifacts, since there is evidence that some CDCs are also able to form arcs under native conditions (reviewed in [27]). Recent experimental work on cells suggests that pores of different sizes can coexist (reviewed in [43]). The questions are, however, whether these structures are functional or not and what their importance is in the mechanism of pathogenesis. Here, the PLM approach could be extremely useful in understanding the molecular details of pore formation, their structure and functionality, and the biophysical properties of the pores. However, only a few PLM studies, on different members of the CDC family, have been reported (Table 1).

4. Overview of existing PLM data on CDC and their implications

PLM studies on CDCs have shown a great variety of events occurring on planar lipid membranes. All reports, save one, show pores with a broad conductance distribution and often three different pore sizes for different CDCs. We use the word ‘pore’ in the

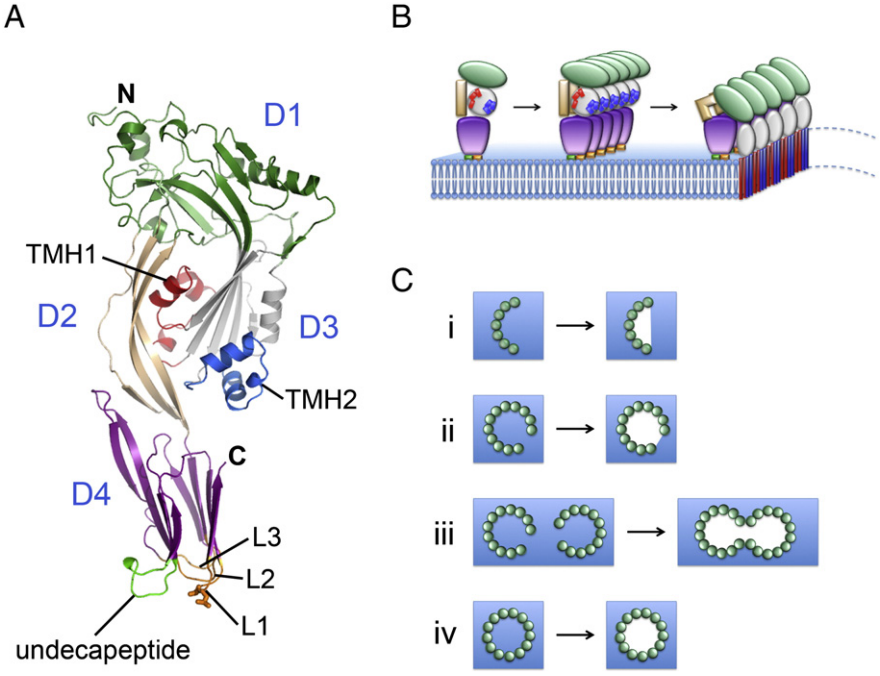

Fig. 2. Structure of a CDC monomer and the proposed mechanism of pore formation. (A) Crystal structure of PFO (PDB-ID 1PFO). Domain D1, green; domain D2, light brown; D3, gray, with TMH1 in red and TMH2 in blue; domain D4, purple, undecapeptide in light green, loops L1–L3 in orange. Residues T490 and L491 – the cholesterol recognition/binding motif in L1 – are shown as orange sticks. N- and C-termini are marked. (B) Schematic representation of pore formation by CDCs based on experimental data. More details regarding steps of pore formation can be found in reviews [23,29,56]. Domains are colored as in (A). First step — monomer binding to the membrane; second step — oligomerization at the membrane (pre-pore complex formation); third step — pore formation, TMH1 (red) and TMH2 (blue) transition from helices (steps 1 and 2) to β-strands (step 3). (C) Schematic representation of formation of pores of different shapes. Blue — membrane, green — CDC oligomer from top, white — pore. (i) small arc pore, (ii) larger arc pore, (iii) double-arc pore, (iv) fully assembled large proteinaceous pore.

Table 1
Results on cholesterol-dependent cytolysins employing the planar lipid bilayer approach.

Protein	Organism	Lipid composition[1]	Bathing solution (concentration in mM)	Conductance distribution	Selectivity	Rectification[2]	Reference
Perfringolysin	*Clostridium perfringens*	PC:Chol (1:1)	KCl 100, 5 Hepes 5 pH 7.0	Broad, 20 ± 12 nS (mean ± SD). Activity inhibited by Zn^{2+}.	nr[4]	nr	[46]
		POPC:Chol (45:55)	NaCl 100, Tris-HCl 10 pH 7.4	Narrow, 4–6 nS for >70% of pores; no pore with conductance < 2.2 nS.	nr	nr	[45]
Pneumolysin	*Streptococcus pneumoniae*	DOPC:ergosterol (1:2)	KCl 100, Hepes 5, EDTA 0.1 pH 7.4	Three pore sizes (conductance, frequency): Small (<50 pS, 48%) Medium (50–1000 pS, + small, 37%)[3] Large (>1 nS, + medium and small, 15%)[3] Activity of small and medium pores inhibited by Ca^{2+} and Zn^{2+}.	 cationic cationic none	 yes none none	[44]
Trp433Phe mutant				Similar to the wild-type pneumolysin			[57]
Sphaericolysin	*Bacillus sphaericus*	POPC:Chol (45:55)	NaCl 100, Tris-HCl 10 pH 7.4	Broad, 2.0 ± 0.6 nS (mean ± SE) Three pore sizes (conductance, frequency[3]): Small (<100 pS) Medium (100–1000 pS) Large (>1 nS, 27%) Slow increases in current with no clear transitions are also present.	nr	nr	[58]
Tetanolysin	*Clostridium tetani*	Oxidized Chol	NaCl 145, Hepes 10 pH 7.4	Broad, main peak at 28 pS. In EggPC:Chol mixtures, membrane ruptures were observed above 30% Chol. No tetanolysin effect below 30% Chol.	cationic	none	[59]
Listeriolysin	*Listeria monocytogenes*	DOPC:Chol (80:20) DOPC:Chol (65:35)	KCl 100, MES 10 pH 5.5 or KCl 100, Hepes 10 pH 7.4	Regardless of pH and lipid composition there are 3 pore sizes (conductance, frequency): Small (<1 nS, >49%) Medium (1–4 nS) Large (>4 nS, 10%) Co-presence of slow increases in current are observed. More pores were observed at pH 5.5 or at higher Chol content.	nr	nr	[48]

[1] Molar composition of the lipid membrane used for the PLM experiment is stated.
[2] Rectification means that the current–voltage curve is non-linear.
[3] The simultaneous presence of smaller-sized channels cannot be excluded in membranes containing medium or large channels.
[4] nr, not reported.

operational sense, to indicate the opening of ion passages in the lipid membrane that result in a particular state, as based on conductance values [27,44]. It is therefore extremely difficult to assign a particular protein assembly to these variously sized pores. Large pores have well defined conductances of more than 1 nS and most probably correspond to barrel-stave pores (Fig. 2C, iii and iv), as proposed for PFO [45]. Medium and small sized pores are quite frequent, constituting up to half of all observed events. In several cases it was possible to inhibit the activity of small pores with certain divalent cations, such as Zn^{2+} or Ca^{2+} [44,46]. As noted by Korchev et al., this could reflect either a blocking of pores or a gating process [44]. However, both are consistent with small sized pores, and PLM ionic currents for other CDCs reflect a very dynamic nature for the pores, which may be consistent with the lipid component of the membrane, as proposed for the arc pores (Fig. 2C, i and ii). Similar behavior was reported recently for the MACPF protein human perforin [47]. From PLM experiments with perforin and LLO ([47,48] and our unpublished observations), it is possible to identify mainly two different pore-forming abilities — a well-defined, step-like increase, compatible with a ring-shaped pore formation (Fig. 2C, iii and iv), and noisier, smaller steps that cannot be related to the defined and compact proteinaceous ring structure. We therefore assign to this last behavior the proteolipidic arc-shaped pore formation model (Fig. 2C, i and ii), which fits better with the noisier signals. In the arc configuration, two features are responsible for the current noise. First, the leaflets of the lipidic portion have to be re-arranged in order to avoid exposure of the hydrophobic chains to the water environment; secondly, the contact surface between the last protein monomer and the lipid connection can result in some leakages that allow ion transfer. Structural studies of the same samples by AFM demonstrated that both pore configurations (rings and arcs) are formed by CDC proteins [39,49], further lending support for the idea that diverse pore structures exist at the surface of the membrane.

PLM studies have been carried out in model membrane systems composed of well-defined lipid composition. However, the lipid composition may significantly affect formation of pores, as recently shown for perforin [47]. The ordering of acyl chains has profound effects on how pores are formed. Perforin inserts more promptly into membranes composed of lipids with less ordered acyl chains (i.e. 1,2-dioleoyl-*sn*-glycero-3-phosphocholine (DOPC) or 1,2-diphytanoyl-*sn*-glycero-3-phosphocholine (DPhPC)). This leads to the formation of smaller pores and unresolved current increases, i.e. no single steps are discriminated, a phenomenon that we assign to the oligomerization process [47]. A sequential addition of monomers on a pre-formed pore configuration (typically arc) increases the dimensions of the pore, which can be visualized as a current increase, step-like or undefined. Membranes composed of more ordered lipids (i.e. 1-palmitoyl-2-oleoyl-*sn*-glycero-3-phosphocholine (POPC)) prevented premature insertion and, hence, preferentially larger pores were observed.

Studies on MAC proteins have demonstrated the increase in conductance of the pores. The sequential addition of C9 subunits to the pre-formed C5b-8 complex has typically been observed as very small steps (around 11 pS) in current [50]. Taken together with the current structural information about MAC proteins [51,52], the initial complex is seen to anchor the structure to the membrane, and only oligomerization of C9 proteins leads to the formation of active pores, confirming the electrophysiological measurements. In the case of CDC, since the new monomer that will bind the pre-existing structure has to re-arrange the α-helices to β-barrels, and since, at the same time, the D2 domain has to collapse, the displacement of the lipid counterpart could not be sharp enough to produce a well-defined step in current. Thus, the unresolved current increases observed could fit quite well with steps in CDC/PFN oligomerization.

The lipid composition of target membranes clearly has an effect on how pores are formed. Tests of the toxin's pore-forming ability on physiologically more relevant model systems are needed to obtain a clearer picture of the process of pore formation by CDCs. Recently, a few patch-clamp studies have been performed to test CDC activity on real biological membranes. According to El-Rachkidy et al. [53], PLY generates multiple conductance pores in the plasma membrane of CHO cells, which can be clustered in three conductance classes with small (<200 pS), medium (200–1000 pS) or large (>1 nS) conductances. Medium pores were the most frequent and the smallest ones were open for short periods of time. These results are perfectly compatible with the data on PLM listed in Table 1 for PLY and other CDCs. A similar classification of pores was proposed for LLO on HEK293 cells [54]. A complex dynamics was observed, since LLO pores were found to be transient and to oscillate between open and closed states. The pores induced Ca^{2+} oscillations, which further modulate cellular signaling and gene expression. A broad distribution of currents for LLO pores was also observed in macrophages in another study [55]. The presence of multiple conductance steps of LLO pores on the cell membrane are, in these cases, multiples of the smallest current amplitude (i.e. 918 pS [54] or 550 pS [55]). The authors noted that the distribution of pore size depends on LLO concentration [54] and on membrane composition [55], parameters that cannot easily be controlled with a cell system. The important role of a model system like PLM is thus to mimic the physiological conditions, allowing a fuller investigation of all the parameters involved in the pore-forming process. Since the large CDC pore heterogeneity visualized by PLM is replicated in cell systems, it is possible that pores of different sizes may have different biological functions, which remains to be investigated.

Acknowledgements

G. A. and M. P. thank the Slovenian Research Agency for financial support. M. D. S. and M. M. thank the Laboratory of Biomolecular Sequence and Structure Analysis for Health (LaBSSAH) for technical support. We also thank Dr. Zdravko Podlesek for the preparation of Fig. 1A and Prof. Roger Pain for the critical reading of the manuscript.

References

[1] M.W. Parker, S.C. Feil, Pore-forming protein toxins: from structure to function, Progress in Biophysics and Molecular Biology 88 (2005) 91–142.
[2] G. Anderluh, J.H. Lakey, Disparate proteins use similar architectures to damage membranes, Trends in Biochemical Sciences 33 (2008) 482–490.
[3] M. Dalla Serra, M. Tejuca, Pore-Forming Toxins, eLS, 2011, http://dx.doi.org/10.1002/9780470015902.a0002655.pub2.
[4] I. Iacovache, F.G. van der Goot, L. Pernot, Pore formation: an ancient yet complex form of attack, Biochimica et Biophysica Acta 1778 (2008) 1611–1623.
[5] M. Dalla Serra, G. Menestrina, Liposomes in the study of pore-forming toxins, Methods in Enzymology 372 (2003) 99–124.
[6] O.S. Mapingire, B. Wager, A.H. Delcour, Electrophysiological characterization of bacterial pore-forming proteins in planar lipid bilayers, Methods in Molecular Biology 966 (2013) 381–396.
[7] M. Dalla Serra, G. Menestrina, Characterization of molecular properties of pore-forming toxins with planar lipid bilayers, Methods in Molecular Biology 145 (2000) 171–188.
[8] S. Zhang, A. Finkelstein, R.J. Collier, Evidence that translocation of anthrax toxin's lethal factor is initiated by entry of its N terminus into the protective antigen channel, Proceedings of the National Academy of Sciences of the United States of America 101 (2004) 16756–16761.
[9] T. Neumeyer, F. Tonello, F. Dal Molin, B. Schiffler, F. Orlik, R. Benz, Anthrax lethal factor (LF) mediated block of the anthrax protective antigen (PA) ion channel: effect of ionic strength and voltage, Biochemistry 45 (2006) 3060–3068.
[10] E.M. Nestorovich, V.A. Karginov, A.M. Berezhkovskii, S.M. Bezrukov, Blockage of anthrax PA63 pore by a multicharged high-affinity toxin inhibitor, Biophysical Journal 99 (2010) 134–143.
[11] P.G. Merzlyak, L.N. Yuldasheva, C.G. Rodrigues, C.M. Carneiro, O.V. Krasilnikov, S.M. Bezrukov, Polymeric nonelectrolytes to probe pore geometry: application to the α-toxin transmembrane channel, Biophysical Journal 77 (1999) 3023–3033.
[12] L.Q. Gu, O. Braha, S. Conlan, S. Cheley, H. Bayley, Stochastic sensing of organic analytes by a pore-forming protein containing a molecular adapter, Nature 398 (1999) 686–690.
[13] J. Clarke, H.C. Wu, L. Jayasinghe, A. Patel, S. Reid, H. Bayley, Continuous base identification for single-molecule nanopore DNA sequencing, Nature Nanotechnology 4 (2009) 265–270.

[14] S. Kumar, C. Tao, M. Chien, B. Hellner, A. Balijepalli, J.W. Robertson, Z. Li, J.J. Russo, J.E. Reiner, J.J. Kasianowicz, J. Ju, PEG-labeled nucleotides and nanopore detection for single molecule DNA sequencing by synthesis, Scientific Reports 2 (2012) 684.
[15] D. Rotem, L. Jayasinghe, M. Salichou, H. Bayley, Protein detection by nanopores equipped with aptamers, Journal of the American Chemical Society 134 (2012) 2781–2787.
[16] C. Shao, B. Sun, D.L. DeVoe, M. Colombini, Dynamics of ceramide channels detected using a microfluidic system, PloS One 7 (2012) e43513.
[17] W. Wang, L. Monlezun, M. Picard, P. Benas, O. Francais, I. Broutin, B. Le Pioufle, Activity monitoring of functional OprM using a biomimetic microfluidic device, Analyst 137 (2012) 847–852.
[18] J.R. Thompson, A.J. Heron, Y. Santoso, M.I. Wallace, Enhanced stability and fluidity in droplet on hydrogel bilayers for measuring membrane protein diffusion, Nano Letters 7 (2007) 3875–3878.
[19] K.T. Sapra, H. Bayley, Lipid-coated hydrogel shapes as components of electrical circuits and mechanical devices, Scientific Reports 2 (2012) 848.
[20] A.J. Heron, J.R. Thompson, B. Cronin, H. Bayley, M.I. Wallace, Simultaneous measurement of ionic current and fluorescence from single protein pores, Journal of the American Chemical Society 131 (2009) 1652–1653.
[21] J.R. Thompson, B. Cronin, H. Bayley, M.I. Wallace, Rapid assembly of a multimeric membrane protein pore, Biophysical Journal 101 (2011) 2679–2683.
[22] A. Fischer, M.A. Holden, B.L. Pentelute, R.J. Collier, Ultrasensitive detection of protein translocated through toxin pores in droplet-interface bilayers, Proceedings of the National Academy of Sciences of the United States of America 108 (2011) 16577–16581.
[23] E.M. Hotze, R.K. Tweten, Membrane assembly of the cholesterol-dependent cytolysin pore complex, Biochimica et Biophysica Acta 1818 (2012) 1028–1038.
[24] S.K. Cassidy, M.X. O'Riordan, More than a pore: the cellular response to cholesterol-dependent cytolysins, Toxins 5 (2013) 618–636.
[25] S. Choi, K.D. Lee, Enhanced gene delivery using disulfide-crosslinked low molecular weight polyethylenimine with listeriolysin o-polyethylenimine disulfide conjugate, Journal of Controlled Release 131 (2008) 70–76.
[26] M. Kullberg, K. Mann, T.J. Anchordoquy, Targeting Her-2+ breast cancer cells with bleomycin immunoliposomes linked to LLO, Molecular Pharmaceutics 9 (2012) 2000–2008.
[27] R.J. Gilbert, M. Mikelj, M. Dalla Serra, C.J. Froelich, G. Anderluh, Effects of MACPF/CDC proteins on lipid membranes, Cellular and Molecular Life Sciences 70 (2013) 2083–2098.
[28] E.M. Hotze, H.M. Le, J.R. Sieber, C. Bruxvoort, M.J. McInerney, R.K. Tweten, Identification and characterization of the first cholesterol-dependent cytolysins from Gram-negative bacteria, Infection and Immunity 81 (2013) 216–225.
[29] R.J. Gilbert, Inactivation and activity of cholesterol-dependent cytolysins: what structural studies tell us, Structure 13 (2005) 1097–1106.
[30] K.S. Giddings, J. Zhao, P.J. Sims, R.K. Tweten, Human CD59 is a receptor for the cholesterol-dependent cytolysin intermedilysin, Nature Structural and Molecular Biology 11 (2004) 1173–1178.
[31] S.E. Gelber, J.L. Aguilar, K.L.T. Lewis, A.J. Ratner, Functional and phylogenetic characterization of vaginolysin, the human-specific cytolysin from *Gardnerella vaginalis*, Journal of Bacteriology 190 (2008) 3896–3903.
[32] S.C. Feil, S. Lawrence, T.D. Mulhern, J.K. Holien, E.M. Hotze, S. Farrand, R.K. Tweten, M.W. Parker, Structure of the lectin regulatory domain of the cholesterol-dependent cytolysin lectinolysin reveals the basis for its Lewis antigen specificity, Structure 20 (2012) 248–258.
[33] J. Rossjohn, S.C. Feil, W.J. McKinstry, R.K. Tweten, M.W. Parker, Structure of a cholesterol-binding, thiol-activated cytolysin and a model of its membrane form, Cell 89 (1997) 685–692.
[34] G. Polekhina, K.S. Giddings, R.K. Tweten, M.W. Parker, Insights into the action of the superfamily of cholesterol-dependent cytolysins from studies of intermedilysin, Proceedings of the National Academy of Sciences of the United States of America 102 (2005) 600–605.
[35] R.W. Bourdeau, E. Malito, A. Chenal, B.L. Bishop, M.W. Musch, M.L. Villereal, E.B. Chang, E.M. Mosser, R.F. Rest, W.J. Tang, Cellular functions and X-ray structure of anthrolysin O, a cholesterol-dependent cytolysin secreted by *Bacillus anthracis*, Journal of Biological Chemistry 284 (2009) 14645–14656.
[36] L. Xu, B. Huang, H. Du, X.C. Zhang, J. Xu, X. Li, Z. Rao, Crystal structure of cytotoxin protein suilysin from *Streptococcus suis*, Protein & Cell 1 (2010) 96–105.
[37] R. Ramachandran, A.P. Heuck, R.K. Tweten, A.E. Johnson, Structural insights into the membrane-anchoring mechanism of a cholesterol-dependent cytolysin, Nature Structural Biology 9 (2002) 823–827.
[38] A.P. Heuck, R.K. Tweten, A.E. Johnson, Assembly and topography of the prepore complex in cholesterol-dependent cytolysins, Journal of Biological Chemistry 278 (2003) 31218–31225.
[39] D.M. Czajkowsky, E.M. Hotze, Z. Shao, R.K. Tweten, Vertical collapse of a cytolysin prepore moves its transmembrane beta-hairpins to the membrane, EMBO Journal 23 (2004) 3206–3215.
[40] N. Lukoyanova, H.R. Saibil, Friend or foe: the same fold for attack and defense, Trends in Immunology 29 (2008) 51–53.
[41] C.J. Rosado, S. Kondos, T.E. Bull, M.J. Kuiper, R.H.P. Law, A.M. Buckle, I. Voskoboinik, P.I. Bird, J.A. Trapani, J.C. Whisstock, M.A. Dunstone, The MACPF/CDC family of pore-forming toxins, Cellular Microbiology 10 (2008) 1765–1774.
[42] R.J. Gilbert, Pore-forming toxins, Cellular and Molecular Life Sciences 59 (2002) 832–844.
[43] M.A. Hamon, D. Ribet, F. Stavru, P. Cossart, Listeriolysin O: the Swiss army knife of Listeria, Trends in Microbiology 20 (2012) 360–368.
[44] Y.E. Korchev, C.L. Bashford, C.A. Pasternak, Differential sensitivity of pneumolysin-induced channels to gating by divalent cations, Journal of Membrane Biology 127 (1992) 195–203.
[45] L.A. Shepard, O. Shatursky, A.E. Johnson, R.K. Tweten, The mechanism of pore assembly for a cholesterol-dependent cytolysin: formation of a large prepore complex precedes the insertion of the transmembrane β-hairpins, Biochemistry 39 (2000) 10284–10293.
[46] G. Menestrina, C.L. Bashford, C.A. Pasternak, Pore-forming toxins: experiments with *S. aureus* alpha-toxin, *C. perfringens* theta-toxin and *E. coli* haemolysin in lipid bilayers, liposomes and intact cells, Toxicon 28 (1990) 477–491.
[47] T. Praper, A. Sonnen, G. Viero, A. Kladnik, C.J. Froelich, G. Anderluh, M. Dalla Serra, R.J. Gilbert, Human perforin employs different avenues to damage membranes, Journal of Biological Chemistry 286 (2011) 2946–2955.
[48] A. Bavdek, R. Kostanjšek, V. Antonini, J.H. Lakey, M. Dalla Serra, R.J. Gilbert, G. Anderluh, pH dependence of listeriolysin O aggregation and pore-forming ability, FEBS Journal 279 (2011) 126–141.
[49] M. Marchioretto, V. Antonini, L. Lunelli, R. Dallapiccola, T. Praper, G. Anderluh, M. Dalla Serra, Membrane composition effects on pore-forming ability of two cholesterol-dependent cytolysins, European Biophysics Journal with Biophysics Letters 40 (Supp 170) (2011).
[50] J.W. Shiver, J.R. Dankert, A.F. Esser, Formation of ion-conducting channels by the membrane attack complex proteins of complement, Biophysical Journal 60 (1991) 761–769.
[51] A.E. Aleshin, I.U. Schraufstatter, B. Stec, L.A. Bankston, R.C. Liddington, R.G. DiScipio, Structure of complement C6 suggests a mechanism for initiation and unidirectional, sequential assembly of membrane attack complex (MAC), Journal of Biological Chemistry 287 (2012) 10210–10222.
[52] M.A. Hadders, D. Bubeck, P. Roversi, S. Hakobyan, F. Forneris, B.P. Morgan, M.K. Pangburn, O. Llorca, S.M. Lea, P. Gros, Assembly and regulation of the membrane attack complex based on structures of C5b6 and sC5b9, Cell Reports 1 (2012) 1–8.
[53] R.G. El-Rachkidy, N.W. Davies, P.W. Andrew, Pneumolysin generates multiple conductance pores in the membrane of nucleated cells, Biochemical and Biophysical Research Communications 368 (2008) 786–792.
[54] H. Repp, Z. Pamukci, A. Koschinski, E. Domann, A. Darji, J. Birringer, D. Brockmeier, T. Chakraborty, F. Dreyer, Listeriolysin of listeria monocytogenes forms Ca2+-permeable pores leading to intracellular Ca2+ oscillations, Cellular Microbiology 4 (2002) 483–491.
[55] H. Zwaferink, S. Stockinger, P. Hazemi, R. Lemmens-Gruber, T. Decker, IFN-beta increases listeriolysin O-induced membrane permeabilization and death of macrophages, Journal of Immunology 180 (2008) 4116–4123.
[56] R.K. Tweten, Cholesterol-dependent cytolysins, a family of versatile pore-forming toxins, Infection and Immunity 73 (2005) 6199–6209.
[57] Y.E. Korchev, C.L. Bashford, C. Pederzolli, C.A. Pasternak, P.J. Morgan, P.W. Andrew, J.T. Mitchell, A conserved tryptophan in pneumolysin is a determinant of the characteristics of channels formed by pneumolysin in cells and planar lipid bilayers, Biochemistry Journal 329 (1998) 571–577.
[58] C. From, P.E. Granum, S.P. Hardy, Demonstration of a cholesterol-dependent cytolysin in a noninsecticidal *Bacillus sphaericus* strain and evidence for widespread distribution of the toxin within the species, FEMS Microbiology Letters 286 (2008) 85–92.
[59] R. Blumenthal, W.H. Habig, Mechanism of tetanolysin-induced membrane damage: studies with black lipid membranes, Journal of Bacteriology 157 (1984) 321–323.